Model-Driven Design of Microwave Filters Based on Scalable Circuit Models

Van Nechel, Evi; Ferranti, Francesco; Rolain, Yves; Lataire, John

Published in:
IEEE Transactions on Microwave Theory and Techniques

DOI:
10.1109/TMTT.2018.2842197

Publication date:
2018

Document Version:
Submitted manuscript

Model-Driven Design of Microwave Filters Based on Scalable Circuit Models

Evi Van Nechel, *Student Member, IEEE*, Francesco Ferranti, *Senior Member, IEEE*, Yves Rolain, *Fellow, IEEE*, and John Lataire, *Member, IEEE*

***Abstract*— Most microwave filters are currently designed using direct electromagnetic (EM) optimization. This method holds several disadvantages regarding the provided physical insight to designers and duration of the optimization process. To circumvent these drawbacks, we propose a filter design based on scalable circuit models. This model-driven design competes with EM optimization by maintaining the accuracy of the optimization results while providing a very significant speedup and gaining physical insight on the EM working mechanism of the filter of interest. This paper discusses the advantages of using the proposed model-driven design by the illustration on a defected ground structure filter. A scalable equivalent circuit model is used in the design procedure to provide physical insight to the designer and to speed up the design process enormously.**

***Index Terms*— Defected ground structure (DGS), efficient design, microwave filter design, scalable circuit models.**

I. Introduction

MICROSTRIP filters are widely used in modern microwave communication systems such as Wi-Fi, 5G, and satellite navigation. This increasingly broad range of applications implies that the frequency spectrum becomes more and more crowded, resulting in more demanding filter specifications. These specifications cannot be fulfilled anymore by using a classical design based on basic, ideal transmission line structures, e.g., a simple delay line, without resorting to an optimization process. The need for more complex transmission line structures and combinations of distributed and discrete components [1] (such as a transmission line that is loaded by a capacitance along the line) increases to deal with these demanding specifications.

The classical filter synthesis procedure [2] is not adapted to the use of more complex transmission line structures and their associated models in the design. It uses idealized circuit models, consisting of ideal and reactive components only. Next, the lumped components are transformed into ideal transmission lines or ideal coupled transmission line sections. The complex structures, however, cannot be approximated by a single ideal element. They require nonideal components and/or subsystems to obtain a good match of the desired and realized frequency response. Approximating these complex structures by the empirical design equations obtained for standard and ideal transmission line structures is too crude. Hence, in the realization phase, the classical design procedure is not sufficiently accurate anymore to realize the required frequency response accurately.

The lack of accuracy of the idealization used in the classical synthesis approach is alleviated using numeric optimization techniques [3]. However, this comes at a high computational cost. The designer is not only forced to use accurate but very time-consuming electromagnetic (EM) simulations but, what is even more important, also loses the physical insight of the link between the transmission line section and the equivalent circuit components that is provided by the classical synthesis approach. This vision about the current way of designing RF filters is also described in [4]. To overcome these disadvantages, we propose a model-driven design based on scalable circuit models.

In this paper, surrogate-assisted techniques for design quantities of interest (e.g., design specifications) [5]–[8] have been proposed for the efficient optimization of computationally expensive models, for example, EM models of filters. In [9], we introduced a filter design by metamodels that work directly on the performance quantities (or the filter specifications) of the filter of interest. It speeds up the design process enormously compared with EM optimization without compromising on the reliability and accuracy of the results. The metamodels are reusable for different filter specifications and can also be used for variability analysis [9]. The approach in [9] solves many drawbacks of EM optimization except one: it does not provide much physical insight to designers. The research of an equivalent circuit model is an important concept in several communities: from filter design to signal and power integrity. The power of an equivalent circuit is used in the core of the design process. Circuit interpretation is very often used to help decide on the layout of a filter, layout corrections for power and signal integrity issues in printed circuit boards and power distribution networks. A physical interpretation allows understanding which kind of phenomena is needed to achieve/suppress resonances, to achieve/suppress certain zeros/poles in the transfer function behavior, and similar design objectives. From a modeling point of view, the circuit representation is not the only one, for example, surrogate

Manuscript received March 1, 2018; revised May 23, 2018; accepted May 24, 2018. Date of publication June 14, 2018; date of current version October 4, 2018. This work was supported in part by the Research Council of the Vrije Universiteit Brussel (SRP 19), in part by the Research Foundation Flanders (FWO-Vlaanderen), and in part by the Flemish Government (Methusalem Fund METH1). This paper is an expanded version of a paper presented at the IEEE MTT-S International Microwave and RF Conference, Ahmedabad, India, December 2017. *(Corresponding author: Evi Van Nechel.)*

E. Van Nechel, Y. Rolain, and J. Lataire are with the Department of Fundamental Electricity and Instrumentation, Vrije Universiteit Brussel, 1050 Brussels, Belgium (e-mail: evi.van.nechel@vub.be; yves.rolain@vub.be; john.lataire@vub.be).

F. Ferranti is with the Institut Mines-Télécom Atlantique, Microwave Department, CNRS UMR 6285 Lab-STICC, 29238 Brest CEDEX 3, France (e-mail: francesco.ferranti@imt-atlantique.fr).

Digital Object Identifier 10.1109/TMTT.2018.2842197

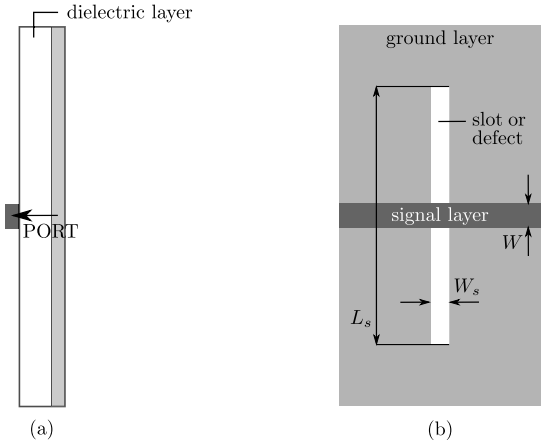

Fig. 1. Layout of the DGS. (a) Cross section. (b) Top view.

models can be built on different design quantities of interest. However, designers often desire a physical interpretation of the EM phenomena, and then, they can really benefit from a circuit model interpretation.

The model-driven design approach that we propose in this paper is based on scalable lumped-element equivalent circuit models. The scalable circuit model is much faster to evaluate when compared with time-consuming EM-simulations, and it is reusable for different filter specifications. Most importantly, it provides physical insight to the designer concerning the EM filter's working mechanism, while EM optimization [3] or metamodeling of performance quantities [9] does not provide this very valuable information. The circuit model needs to be scalable, which is useful in a filter design. As scalable, we intend that the circuit parameters of the equivalent circuit are linked to the design parameters by a set of mathematical functions.

A defected ground structure (DGS) filter, described in Section II, is used as a design example. Section III describes an innovative equivalent circuit model of the DGS and how it is obtained. Section IV discusses the design procedure based on scalable circuit modeling and apply it on a 4-D design space example. Section V gives a qualitative as well as a quantitative comparison between the proposed approach and the EM simulation-based optimization approach. Conclusions are drawn in Section VII.

II. DGS

This section shortly discusses the DGS we used as a design example. A DGS is a microstrip filter that consists of a transmission line on the top layer with one or more resonating slots (called "defects") in the ground plane. The resonating property of the slots implies that the DGS behaves as a bandstop filter.

The slots can take different shapes [10]. In our case, the defect in the ground plane is a rectangular slot positioned perpendicularly to and symmetrically around the transmission line (Fig. 1).

The DGS has three geometrical design parameters: the width of the transmission line, W, and the width and length of the slotline, W_s and L_s. Also, as explained in what follows, we have added another design parameter, namely, the relative permittivity of the substrate ε_r.

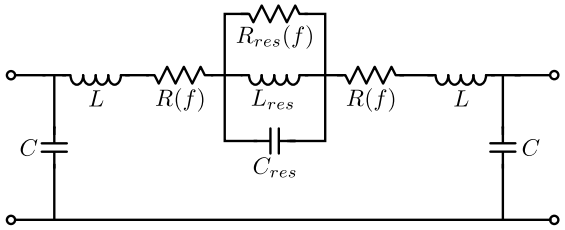

Fig. 2. Circuit model with frequency-dependent resistive elements.

III. Novel Equivalent Circuit Model

We identify a novel equivalent circuit model structure for the filter to be designed, in this case a DGS. In this section, we describe the extracted circuit model for the DGS in detail. This equivalent circuit is able to represent the EM behavior of the filter with high accuracy.

The proposed circuit model (see Fig. 2) can be split in two parts: a part that represents the transmission line and a part that represents the slot of the DGS. The transmission line is represented by Telegrapher's equation representation [L, C, and $R(f)$] [11]. The shunt conductance, G, is not modeled here, because the dielectric losses are negligible with respect to the conductor losses and radiation losses. The slot is represented by an RLC-resonator [L_{res}, C_{res}, and $R_{\text{res}}(f)$] of which the resistor is frequency-dependent.

This circuit model builds up on different existing circuits from the literature and provides additional circuit elements that highly improve the accuracy of the equivalent circuit. In [12]–[14], an LC resonator is proposed to model the slot. In order to use the circuit model in the filter design process, the model should be very accurate. To obtain a higher accuracy, it is necessary to introduce losses into the model. Figs. 3 and 4 show the amplitude and phase responses of the simulated S_{11} and the S_{12} parameters of the lossless circuit model (model of Fig. 2 without resistive elements) (dark gray dashed line) and of the EM DGS structure (full black line, EM simulation). The model error is shown in dark gray. The error of the circuit model needs to be reduced to consider the equivalent circuit for filter design purposes. Including losses in the circuit model will sufficiently lower the model error.

The losses present in the DGS can be conductor losses, due to the skin effect, and more importantly radiation losses in the slot. In the literature, many references exist where losses have been taken into account [15]–[17]. The losses introduced in these references are independent of the frequency. However, both conductor losses [11] as well as radiation losses of the slot are frequency-dependent [18], [19]. Figs. 3 and 4 also confirm the need of frequency-dependent losses: the model error of the lossless model increases with the frequency.

The losses introduced by the skin effect depend on the frequency in square-root-sense [11]. Therefore, the conductor losses are introduced into the circuit model (see Fig. 2) by a

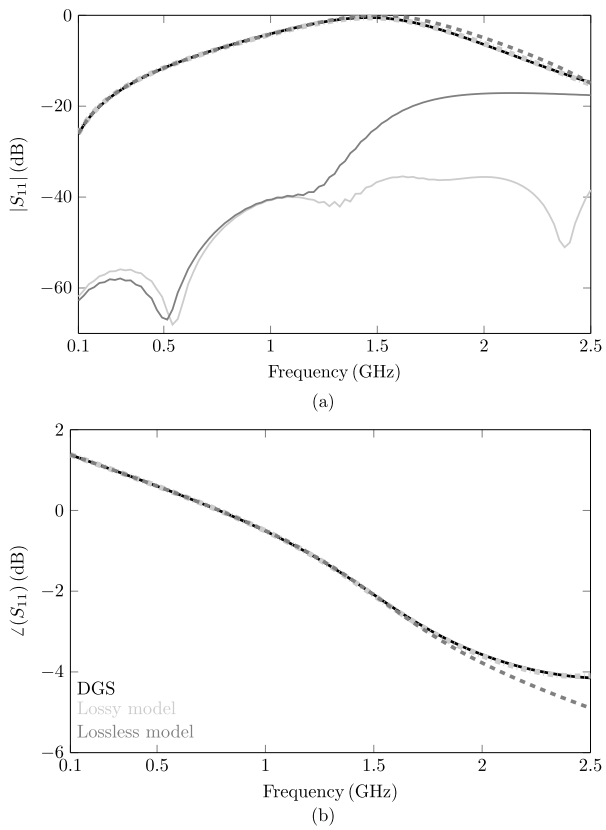

Fig. 3. Comparison of the S_{11} parameter of the simulated DGS (full black line, EM simulation), the lossless circuit model (dark gray dashed line), and the final circuit model with losses (light gray dashed line). The model error is shown in dark and light gray for the lossless and lossy circuit model, respectively. (a) Amplitude response. (b) Phase response.

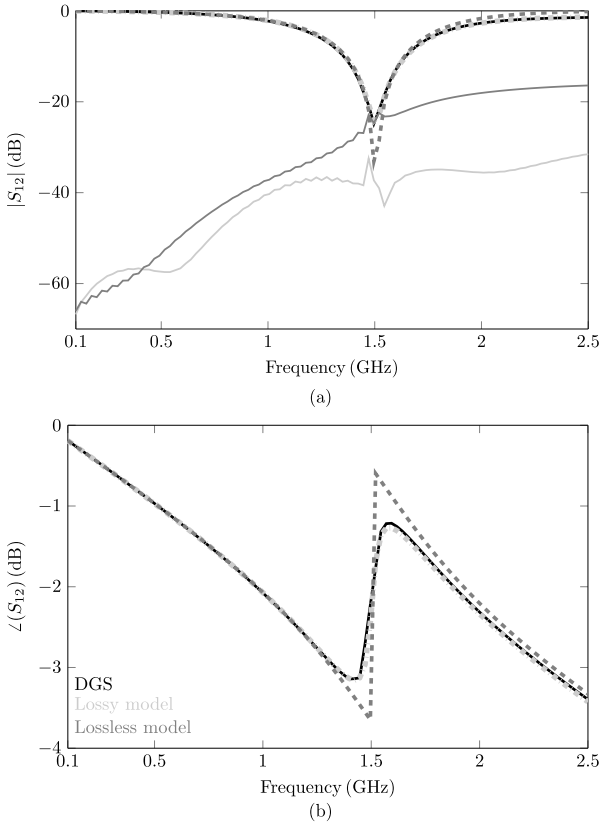

Fig. 4. Comparison of the S_{12} parameter of the simulated DGS (full black line, EM simulation), the lossless circuit model (dark gray dashed line), and the final circuit model with losses (light gray dashed line). The model error is shown in dark and light gray for the lossless and lossy circuit model, respectively. (a) Amplitude response. (b) Phase response.

resistor

$$R(f) = R_{\text{cond}}\sqrt{f}. \tag{1}$$

The radiation losses of the slot are introduced in the model by using a frequency-dependent resistive element. To this end, a resistor, $R_{\text{res}}(f)$, is connected in parallel with the LC-resonator (see Fig. 2). $R_{\text{res}}(f)$ is defined as

$$R_{\text{res}}(f) = R_{\text{rad}} \cdot \left(\frac{f}{f_0}\right)^{\alpha}. \tag{2}$$

It consists of a frequency independent parameter R_{rad} that is multiplied by the normalized frequency. Since the dependence in frequency is related to some design parameters (the length and the width of the slot), it cannot be fixed when used in a filter design. Therefore, it is modeled by a coefficient α.

Figs. 3 and 4 show the amplitude and phase responses of the simulated S_{11} and the S_{12} parameters of the final circuit model with losses (as shown in Fig. 2) (light gray dashed line) and of the EM DGS structure (full black line, EM simulation). The model error of the equivalent circuit (full light gray) is now small enough over the whole frequency band of interest.

We briefly discuss a first step that can be taken to generalize the circuit model in case the user wants to design a DGS with multiple slots. An extra slot introduces an extra resonance in the frequency response function (FRF). To model this effect, an extra LC-resonator can simply be added to the circuit model. To model the phase correctly, a delay line should be added between two consecutive LC-resonators to model the transmission line between the two consecutive slots in the DGS. Should the user desire a fully lumped-circuit model, the transmission lines can be approximated by equivalent lumped circuits.

To use the proposed equivalent circuit model in the filter design, we need to make the circuit model scalable. Therefore, the circuit parameters of the model need to be related to the design parameters of the filter structure by mathematical functions. The generation of these so-called scalable circuit models is described in Section IV-B. The use of these scalable circuit models in a filter design is validated in Section V.

IV. Filter Design by Scalable Circuit Modeling

In [9], we proposed metamodels of filter performance quantities to speed up the optimization and variability analysis tasks of the filter design flow. This filter design approach has several advantages over design by EM-based optimization. Metamodels speed up the design process drastically and are reusable for different filter specifications. For the EM-based optimization, this technique is also accurate but unfortunately it does not give much more physical insight to designers.

In this paper, we propose a new approach that, besides the advantages of very efficient design tasks, also provides physical insight in the design by the use of a scalable equiv-

TABLE I

WE USED FIVE DGS DESIGN CASES WITH DIFFERENT FILTER SPECIFICATIONS TO VALIDATE THE PROPOSED DESIGN BASED ON SCALABLE CIRCUIT MODELING

	Case 1	Case 2	Case 3	Case 4	Case 5
Center, f_0 (GHz)	1.37	1.25	1.50	1.18	1.65
Cut-off 1, fc_1 (GHz)	0.88	0.65	1.00	0.69	1.18
Cut-off 2, fc_2 (GHz)	1.89	1.90	2.10	1.70	2.22
$\|S_{21}\|@f_0$ (dB)	−24.0	−28.0	−22.0	−24.0	−18.0

alent circuit model. We validate the proposed filter design approach using the DGS example described in Section II with the corresponding novel equivalent circuit model described in Section III. Like design by metamodeling [9], this approach requires some user interaction. Section IV-A explains how the user settings are selected. Section IV-B describes the generation of a scalable circuit model. Three different sets of filter specifications (see Table I) are the goal of multiple optimizations. Section V describes the numerical results.

We performed all EM simulations via the momentum simulator in ADS2014. We used a substrate with $\tan(\delta) = 0.0022$ and a dielectric height $h = 1.524$ mm. As previously mentioned, we used the relative permittivity of the substrate ε_r as a design parameter (see Section IV-A).

A. User Settings

The user needs to define the frequency range and the design space. We simulated the S-parameter data over a frequency range of 0.1–2.5 GHz for 241 equidistant frequency samples. The design parameters can be geometrical parameters as well as material properties. In the numerical example of [9], only two geometrical parameters were considered as design parameters: W_s and L_s, respectively, the width and length of the slotline (see Fig. 1). In this paper, we opt for a more complex 4-D design space, including the width of the transmission line, W (see Fig. 1), and the relative permittivity of the substrate, ε_r along with W_s and L_s.

These design parameters should be bounded. Large W_s values lead to high reflections in the passband, suppressing the wanted frequencies too much. Small values are not physically realizable. Large L_s values make the size of the PCB become too large. Small L_s values would bring the center frequency f_0 outside the frequency range of interest, since $f_0 \propto (1/L_s)$. For large W values, the characteristic impedance Z_0 no longer decreases significantly. Small values are not physically realizable. Concerning ϵ_r, a range was selected that is commonly used in microwave applications.

The boundaries of the design parameters indirectly determine the feasible filter specifications (f_0, fc_1, fc_2, and $|S_{21}|@f_0$) (see Table II).

B. Generation of a Scalable Circuit Model

As described in Section IV-A, we chose a 4-D design space with design parameters: W, W_s, L_s, and ϵ_r. The circuit model is composed of seven circuit parameters: L, C, R_{cond}, R_{rad}, α, L_{res}, and C_{res} (see Section III). However, some circuit parameters can be fixed to lower the degrees of freedom.

TABLE II

DESIGN SPACE NEEDS TO BE LIMITED BY THE USER. THE BOUNDARIES OF THE DESIGN SPACE INDIRECTLY DETERMINE THE FEASIBLE FILTER SPECIFICATIONS

Design parameters	min	max
TL width, W (mm)	1.80	5.80
Slotline width, W_s (mm)	1.00	5.00
Slotline length, L_s (mm)	80.0	100.0
Relative permittivity, ε_r	1.50	6.50

Feasible filter specifications	min	max
Center frequency, f_0 (GHz)	1.13	1.71
Cut-off frequency 1, fc_1 (GHz)	0.63	1.24
Cut-off frequency 2, fc_2 (GHz)	1.46	2.5
$\|S_{21}\|@f_0$ (dB)	−34	−18.7

The capacitance C represents the capacitance between the two substrate conductor layers. Since the thickness of the substrate, h, is not considered as a design parameter, C can be fixed. R_{cond} represents the conductor losses. Within the chosen design space, the conductor losses did not change significantly. Therefore, R_{cond} could also be fixed. Finally, the circuit model is composed of five circuit parameters: L, R_{rad}, α, L_{res}, and C_{res}.

Different sampling techniques exist to select a set of design space samples to which corresponds a set of circuit element values used as data sample to build the scalable circuit model. For example, Latin hypercube design [20] and quasi-random sequences [21]. Sobol and Halton sequences [21] are famous among quasi-random sequences. In this paper, we have chosen the Sobol quasi-random sequence scheme [21]. Simple sampling schemes, such as a regular tensor-product sampling, will immediately provide a high number of design samples as soon as the number of dimensions of the design space increases. Let us imagine to have M design parameters and to sample each design parameters interval with L samples. By taking the combination of all these samples (tensor-product), the total number of samples is equal to L^M. This is clearly not an efficient sampling scheme. In this paper, we have used 100 samples within the design space (W, W_s, L_s, and ϵ_r) chosen by a Sobol quasi-random sequence scheme. We note that the sampling can be implemented in an iterative way [22] (adaptive sampling) instead of deciding a fixed number of samples.

Before generating the scalable circuit model, we computed the S-parameter data over 241 frequency samples at each of the 100 design space samples by using momentum. Then, the circuit parameters were optimized in order to match the FRF of the circuit model with the EM simulation-based FRF of the DGS for each of the 100 design space samples. The optimization function *lsqnonlin* was used in MATLAB R2014a. This step provides the circuit element values used as a data sample to build the scalable circuit model.

The scalable circuit model is based on the use of a tessellation-based linear interpolation. Before performing the multidimensional interpolation process based on the previously described data samples, the design space is divided into cells

using simplices [23]. This process is called tessellation, and in this paper, we use the Delaunay tessellation [23]. A simplex is the N-D analog of a triangle in 2-D, and it has $N+1$ vertices. We indicate a simplex region of the design space as Ω_i, $i = 1, \ldots, P$ (P is the total number of simplices after the tessellation) and the corresponding $N+1$ vertices as $\vec{g}_k^{\Omega_i}$, $k = 1, \ldots, N+1$, where $\vec{g}$ denotes the vector of the design parameters. Once the tessellation of the design space is performed, a tessellation-based linear interpolation is used to build the scalable circuit model. A linear interpolation is carried out inside a simplex using barycentric coordinates [24] as interpolation functions. A model based on this interpolation scheme for the 4-D design space composed of $\vec{g} = (W, W_s, L_s, \epsilon_r)$ can be written as

$$\mathbf{Model}(\vec{g}) = \sum_{k=1}^{\mathrm{N+1}} \mathbf{Data}\left(\vec{g}_k^{\Omega_i}\right) \ell_k^{\Omega_i}(\vec{g}) \tag{3}$$

where Ω_i is the simplex that contains the general point $\vec{g}$ and $\ell_k^{\Omega_i}(\vec{g})$ are the corresponding barycentric coordinates.

Other modeling techniques could be used to build scalable circuit models, such as Kriging [7], and polynomial and radial basis functions [25]. We note that when the number of design parameters increases, the curse of dimensionality issue, related to an exponential growth of the design space with its dimensionality, needs to be taken into account. Advanced techniques, such as design space reduction [26] or segmentation [27], can be used.

To validate the quality of the scalable circuit model, of all the 100 EM simulations (all samples in the design space), a part is used to build the scalable model (estimation) and another part is used to validate this model (validation). A scheme inspired by k-fold cross validation is used to subdivide estimation and validation samples in the design space [28]. The set of Q simulations is randomly partitioned into k sets of approximately equal size. Then, for $i = 1, \ldots, k$, a scalable model is built considering all but the ith data partition and the excluded data set is used to evaluate the corresponding validation model error. An average validation model error based on the validation model errors of all the k iterations is used to estimate the average error over the design space for the scalable model built by using all 100 data samples [28]. A tenfold ($k = 10$) cross validation has been used in this paper.

C. DGS Design Using Scalable Circuit Models

When designing a filter, we start from certain filter specifications. A filter design using scalable circuit models basically resolves the same main optimization problem as the EM-based optimization: the goal of the optimization is to find the optimal design parameters values (values of W, W_s, L_s, and ϵ_r in our case), such that the filter response fulfills the required filter specifications. However, in our newly proposed approach, the scalable circuit model is used in the optimization process, while in the EM-based optimization, the structure of interest, in this case the DGS, is optimized by means of EM simulations. A scalable circuit model is much cheaper to evaluate than the very time-consuming EM simulations, which allows speeding up the design process significantly.

TABLE III
PROPOSED CIRCUIT MODELING-BASED DESIGN OPTIMIZATION APPROACH PROVIDES THE DESIRED RESULTS. THE INITIAL AND OPTIMAL VALUES OF THE DESIGN PARAMETERS ARE GIVEN

Initial	Case 1	Case 2	Case 3	Case 4	Case 5
W (mm)	2.59	4.70	5.25	3.82	5.04
W_s (mm)	4.61	3.40	1.11	4.05	3.99
L_s (mm)	90.7	170	123	92.6	82.4
ε_r	5.75	5.46	3.53	1.95	4.12

Optimal	Case 1	Case 2	Case 3	Case 4	Case 5
W (mm)	4.67	5.27	5.35	4.08	3.32
W_s (mm)	1.93	3.44	1.73	2.00	2.73
L_s (mm)	90.7	93.8	91.3	92.6	82.4
ε_r	3.69	5.47	2.06	6.03	1.99

We designed three DGS with different filter specifications given in Table I. The optimization function *patternsearch* was used in MATLAB R2014a for the filter optimization based on the use of the scalable circuit model. This model is able to generate the S-parameters FRF of the filter over the complete design space and frequency range of interest.

V. NUMERICAL RESULTS AND COMPARISON

This section compares the results of the optimization based on the scalable circuit model and the EM-based optimization and it discusses the advantages of the novel proposed approach. All experiments were performed in a Windows environment with 8-GB RAM and Intel Core i7-4770 CPU @ 3.40 GHz.

Table III gives the initial and optimal design parameters values for the five optimization cases. The initial design parameters values were randomly generated within the 4-D design space (bounds of the design space in Table II). Figs. 5–9 show the optimization results for the five design cases.

These results confirm the high accuracy achieved by the proposed design techniques based on a physically interpretable and scalable circuit model. The circuit and EM response of the optimal designs fulfill the required filter specifications for each of the five cases. In what follows, a detailed discussion concerning computational resources for the obtained results will be provided.

Circuit modeling-based optimization is much faster than EM-based optimization. The average CPU time required for one frequency-domain EM simulation (one EM simulation at one point in the design space) over 241 frequency samples is 70 s. The evaluation of the FRF (at one point in the design space) of the scalable circuit model takes only 50 ms on average. Multiplying this CPU time by the number of function evaluations (feval in Table IV) gives us the results shown in Table IV. This confirms the significant computational resources that are saved by using the proposed scalable circuit modeling technique with respect to the EM-based optimization for which one function evaluation would require 70 s.

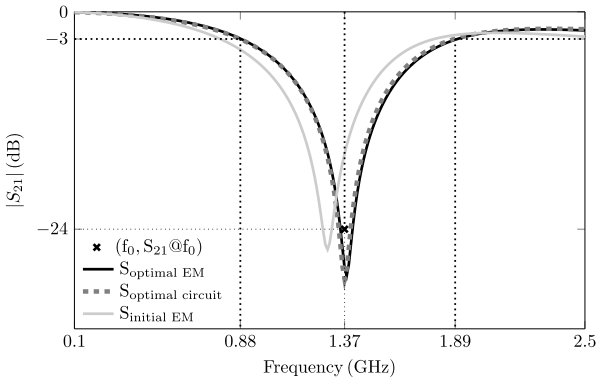

Fig. 5. Design results for the filter specifications of Case 1 (see Table I). Black dots: filter specification template for Case 1. Full black line: FRF of the EM simulation for optimal design parameters values. Dark gray dashed line: FRF of the circuit model for optimal design parameters values. Light gray line: FRF of the EM simulation for initial design parameters values.

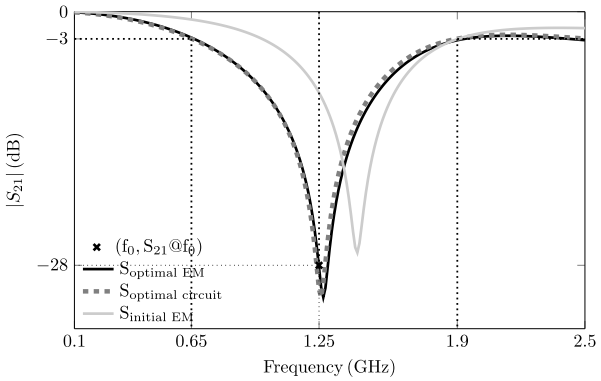

Fig. 6. Design results for the filter specifications of Case 2 (see Table I). Black dots: filter specification template for Case 2. Full black line: FRF of the EM simulation for optimal design parameters values. Dark gray dashed line: FRF of the circuit model for optimal design parameters values. Light gray line: FRF of the EM simulation for initial design parameters values.

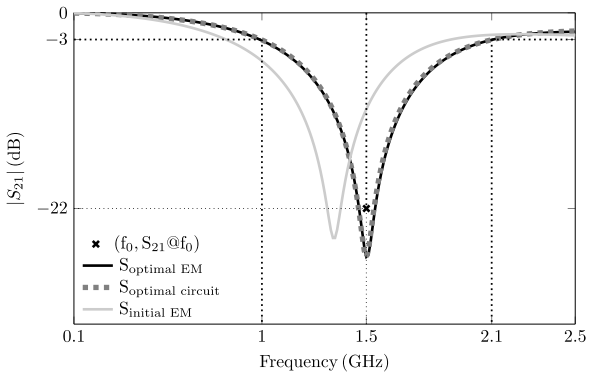

Fig. 7. Design results for the filter specifications of Case 3 (see Table I). Black dots: filter specification template for Case 3. Full black line: FRF of the EM simulation for optimal design parameters values. Dark gray dashed line: FRF of the circuit model for optimal design parameters values. Light gray line: FRF of the EM simulation for initial design parameters values.

Generating the scalable circuit model requires a certain amount of CPU time, due to the acquisition of the 100 EM simulations of 70 s each to generate the S-parameters over 241 frequency samples for all the 100 design space samples. This computational cost is needed to generate data samples needed for the construction of the scalable circuit model. After this

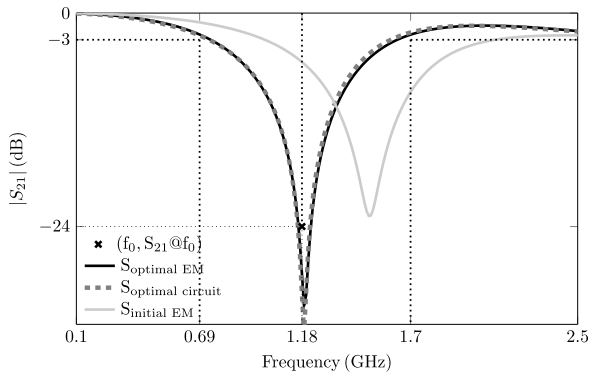

Fig. 8. Design results for the filter specifications of Case 4 (see Table I). Black dots: filter specification template for Case 4. Full black line: FRF of the EM simulation for optimal design parameters values. Dark gray dashed line: FRF of the circuit model for optimal design parameters values. Light gray line: FRF of the EM simulation for initial design parameters values.

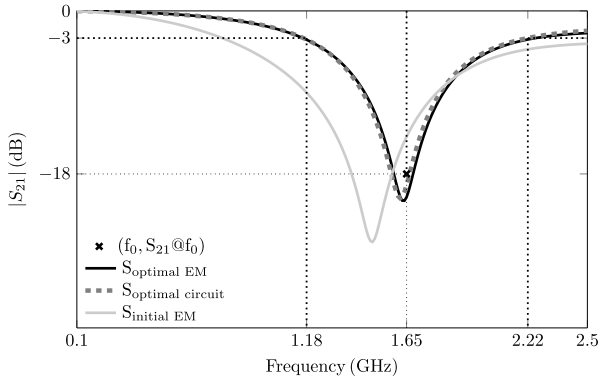

Fig. 9. Design results for the filter specifications of Case 5 (see Table I). Black dots: filter specification template for Case 5. Full black line: FRF of the EM simulation for optimal design parameters values. Dark gray dashed line: FRF of the circuit model for optimal design parameters values. Light gray line: FRF of the EM simulation for initial design parameters values.

TABLE IV
TOTAL OPTIMIZATION TIME USING THE SCALABLE CIRCUIT MODEL WHEN ONE FUNCTION EVALUATION (FEVAL) OF THE SCALABLE CIRCUIT MODEL AT ONE POINT IN THE DESIGN SPACE TAKES 50 ms

	Case 1	Case 2	Case 3	Case 4	Case 5
Fevals	2073	1046	2319	1352	1410
CPU time/feval	x 50 ms	x 50 ms	x 50 ms	x 50 ms	x 50 ms
Total time	104 s	52.3 s	116 s	67.6 s	70.5 s

data generation, the CPU time needed for the extraction of the scalable circuit model is negligible with respect to the CPU time needed to simulate the S-parameter data at the 100 design space samples. Hence, the total CPU time for generating the scalable circuit model is 116.6 min. Once the scalable circuit model is generated, it can be reused in multiple optimization cases, speeding up the filter design tremendously. Table IV gives the total optimization CPU time required in each of the five optimization cases. In all five cases, the required CPU time is much less than the CPU time that EM-based optimization would need considering the high number of function evaluations (2073, 1046, 2319, 1352, and 1410) required by the optimizations. Each function evaluation

corresponds to a filter response evaluation at one point in the design space. Hence, the CPU time needed to generate the scalable circuit model (116.6 min, 100 design space samples) can be definitely accepted considering the saved computational resources in multiple optimization cases.

Besides, the CPU time needed to generate the scalable circuit model can be reduced. A less dense frequency grid can be used to simulate the DGS at the 100 design space samples. The vector fitting method [29] can then be used to evaluate the obtained S-parameter data over a more dense frequency grid. This technique was used and described in [9]. A second way to decrease this initial computational effort is to use adaptive frequency sampling when simulating the S-parameters with the EM solver.

VI. Generalization of the Proposed Design Method

The methodology described in this paper can be generalized for any microwave filter design. We note that when another filter structure (different from the one used in this paper) is designed using the proposed approach, an accurate equivalent circuit model should be at disposal or should be defined as done in this paper. Defining a new circuit model for a new filter structure requires some engineering work. However, this only needs to be done once for one specific filter structure. This is an effort that is worth paying when we consider the enormous amount of time and physical insight that is gained once the model is obtained.

In general, an EM response can be represented by a lumped equivalent circuit model. Specific filter structures will require specific circuit models. The equivalent circuit used in this paper to model a DGS is based on modeling a resonating structure. Hence, this circuit can be used as a basis model when one wants to model other resonating structures. Obviously, also nonresonating structures can be modeled by equivalent circuits.

VII. Conclusion

The model-driven design approach that we have discussed is based on a physically interpretable and scalable lumped-element equivalent circuit model. This type of model is very efficient and accurate and allows a valuable physical insight into the EM working mechanism of the filters. Physical insight is very precious to designers. The numerical results have confirmed the speedup and accuracy provided by the proposed approach with respect to a direct EM simulation-based optimization process.

References

[1] R. Levy, "A new class of distributed prototype filters with applications to mixed lumped/distributed component design," *IEEE Trans. Microw. Theory Techn.*, vol. MTT-18, no. 12, pp. 1064–1071, Dec. 1970.

[2] R. J. Cameron, C. M. Kudsia, and R. Mansour, *Microwave Filters for Communication Systems*. Hoboken, NJ, USA: Wiley, 2015.

[3] S. Bila *et al.*, "Direct electromagnetic optimization of microwave filters," *IEEE Microw. Mag.*, vol. 2, no. 1, pp. 46–51, Mar. 2001.

[4] D. Swanson and G. Macchiarella, "Microwave filter design by synthesis and optimization," *IEEE Microw. Mag.*, vol. 8, no. 2, pp. 55–69, Apr. 2007.

[5] J. W. Bandler *et al.*, "Space mapping: The state of the art," *IEEE Trans. Microw. Theory Techn.*, vol. 52, no. 1, pp. 337–361, Jan. 2004.

[6] N. V. Queipo, R. T. Haftka, W. Shyy, T. Goel, R. Vaidyanathna, and P. K. Tucker, "Surrogate-based analysis and optimization," *Prog. Aerosp. Sci.*, vol. 41, no. 1, pp. 1–28, Jan. 2005.

[7] A. I. J. Forrester and A. J. Keane, "Recent advances in surrogate-based optimization," *Prog. Aerosp. Sci.*, vol. 45, pp. 50–79, Jan./Apr. 2009.

[8] S. Koziel and A. Bekasiewicz, "Rapid microwave design optimization in frequency domain using adaptive response scaling," *IEEE Trans. Microw. Theory Techn.*, vol. 64, no. 9, pp. 2749–2757, Sep. 2016.

[9] E. Van Nechel, F. Ferranti, J. Lataire, and Y. Rolain, "Efficient design optimization and variability analysis of defected ground structure filters using metamodels," in *IEEE MTT-S Int. Microw. RF Conf. (IMaRC)*, Ahmedabad, India, Dec. 2017, pp. 1–4.

[10] G. Breed, "An introduction to defected ground structures in microstrip circuits," *High Freq. Electron.*, vol. 7, pp. 50–52, Nov. 2008.

[11] J. He, N. S. Nahman, and S. M. Riad, "A causal skin-effect model of microstrip lines," in *IEEE MTT-S Int. Microw. Symp. Dig.*, Jun. 1993, pp. 865–868.

[12] A. Boutejdar and A. Omar, "Improvement of compactness of low pass and band pass filter using a simple combination of cross-defected ground structure and a discontinuous microstrip line," *Microw. Opt. Technol. Lett.*, vol. 51, no. 5, pp. 1191–1195, 2009.

[13] D. Ahn, J. S. Park, C. S. Kim, J. Kim, Y. Qian, and T. Itoh, "A design of the low-pass filter using the novel microstrip defected ground structure," *IEEE Trans. Microw. Theory Techn.*, vol. 49, no. 1, pp. 86–93, Jan. 2001.

[14] J.-S. Hong and B. M. Karyamapudi, "A general circuit model for defected ground structures in planar transmission lines," *IEEE Microw. Wireless Compon. Lett.*, vol. 15, no. 10, pp. 706–708, Oct. 2005.

[15] A. M. E. Safwat, F. Podevin, P. Ferrari, and A. Vilcot, "Tunable bandstop defected ground structure resonator using reconfigurable dumbbell-shaped coplanar waveguide," *IEEE Trans. Microw. Theory Techn.*, vol. 54, no. 9, pp. 3559–3564, Sep. 2006.

[16] D.-J. Woo, T.-K. Lee, J.-W. Lee, C.-S. Pyo, and W.-K. Choi, "Novel U-slot and V-slot DGSs for bandstop filter with improved Q factor," *IEEE Trans. Microw. Theory Techn.*, vol. 54, no. 6, pp. 2840–2847, Jun. 2006.

[17] M. K. Mandal and S. Sanyal, "A novel defected ground structure for planar circuits," *IEEE Microw. Wireless Compon. Lett.*, vol. 16, no. 2, pp. 93–95, Feb. 2006.

[18] C. Poschalko and S. Selberherr, "Calculation of the radiation from the slot of a slim enclosure with a cavity resonator model," in *Proc. Asia–Pacific Symp. Electromagn. Compat.*, May 2008, pp. 622–625.

[19] K. Yoshitomi, "Radiation from a slot in an impedance surface," *IEEE Trans. Antennas Propag.*, vol. 49, no. 10, pp. 1370–1376, Oct. 2001.

[20] W.-L. Loh, "On latin hypercube sampling," *Ann. Statist.*, vol. 24, no. 5, pp. 2058–2080, 1996.

[21] P. Brandimarte, *Low-Discrepancy Sequences*. Hoboken, NJ, USA: Wiley, 2014, pp. 379–401.

[22] G. G. Wang and S. Shan, "Review of metamodeling techniques in support of engineering design optimization," *J. Mech. Des.*, vol. 129, no. 4, pp. 370–380, 2007.

[23] D. F. Watson, "Computing the n-dimensional Delaunay tessellation with application to Voronoi polytopes," *Comput. J.*, vol. 24, no. 2, pp. 167–172, Feb. 1981.

[24] D. F. Watson, *Contouring: A Guide to the Analysis and Display of Spatial Data*. New York, NY, USA: Pergamon, 1992.

[25] J. P. Kleijnen, *Design and Analysis of Simulation Experiments*. New York, NY, USA: Springer, 2008.

[26] S. Koziel, A. Bekasiewicz, and W. Zieniutycz, "Expedited EM-driven multiobjective antenna design in highly dimensional parameter spaces," *IEEE Antennas Wireless Propag. Lett.*, vol. 13, pp. 631–634, 2014.

[27] P. Lollini, A. Bondavalli, and F. D. Giandomenico, "A decomposition-based modeling framework for complex systems," *IEEE Trans. Rel.*, vol. 58, no. 1, pp. 20–33, Mar. 2009.

[28] T. Hastie, R. Tibshirani, and J. Friedman, *The Elements of Statistical Learning: Data Mining, Inference, and Prediction* (Springer Series in Statistics), 2nd ed. Springer, 2009.

[29] B. Gustavsen and A. Semlyen, "Rational approximation of frequency domain responses by vector fitting," *IEEE Trans. Power Del.*, vol. 14, no. 3, pp. 1052–1061, Jul. 1999.

Authors' photographs and biographies not available at the time of publication.